OL | Organic Letters

Letter

Cite This: Org. Lett. XXXX, XXX, XXX−XXX

pubs.acs.org/OrgLett

Tunable *E*−*Z* Photoisomerization in α,β-Peptide Foldamers Featuring Multiple (*E*/*Z*)-3-Aminoprop-2-enoic Acid Units

Giulia Marafon,[†] Marco Crisma,[‡] and Alessandro Moretto*[,†,‡]

[†]Department of Chemical Sciences, University of Padova, 35131 Padova, Italy

[‡]Institute of Biomolecular Chemistry, Padova Unit, CNR, 35131 Padova, Italy

Supporting Information

ABSTRACT: Systems in which an external stimulus elicits a response through some sort of modification at the molecular or supramolecular level bear potential for the development of smart materials and devices. This work describes a versatile synthetic approach suitable for the stepwise incorporation of multiple, even consecutive, units of the simplest $C^{\alpha,\beta}$-unsaturated β-amino acid, (*E*/*Z*)-3-aminoprop-2-enoic acid, in peptide-based foldamers. The properties of these, including photoinduced *E*/*Z* isomerizations, were investigated.

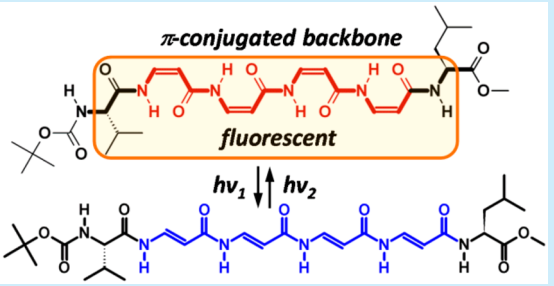

Foldamers are oligomeric molecules based on building blocks other than those characterizing naturally occurring biopolymers, able to highly populate a specific conformation, thus giving rise to a stable and well-defined three-dimensional (3D) architecture.[1] Peptides based on β-amino acids, γ-amino acids, and noncoded α-amino acids, aromatic oligoamides, azapeptides, and oligoureas are among the most extensively investigated classes of compounds in this area.[2] The possibility of triggering the switch of a foldamer between two distinct but structurally defined states (for such systems, the term "dynamic foldamers" has been coined)[3] may offer interesting opportunities. For example, a foldamer undergoing elongation and contraction of its end-to-end distance resulting from the transition between two conformations, each characterized by a different pitch, can be viewed as a molecular spring.[4] Moreover, a conformational transition can convey chemical information across the entire length of a foldamer from a signaling unit at one end to a reporter at the other end, even at multinanometer distances.[5] In this regard, we exploited the (*E*)-fumaramide/(*Z*)-maleamide photoswitchable system as a linker between a chiral and an achiral helical peptide foldamer segment to turn on−off transmission of stereochemical information (a preferred helical screw sense) to the latter.[6] However, such an approach results in the antiverse orientation of the two peptide chains connected to the linker. We therefore became interested in developing peptide-based foldameric systems in which the photoswitchable unit itself would be an amino acid.[7] For this aim, we selected (*E*/*Z*)-3-aminoprop-2-enoic acid [or (*E*/*Z*)-3-aminoacrylic acid]. Considering this β-amino acid as the $C^{\alpha,\beta}$-unsaturated analogue of β-alanine (β-Ala) and exploiting the Δ^E/Δ^Z terminology commonly used for $C^{\alpha,\beta}$-didehydro analogues of protein amino acids, we abbreviate the *E* and *Z* isomers of 3-aminoprop-2-enoic acid as Δ^EβAla and Δ^ZβAla, respectively. We recently succeeded in introducing Δ^ZβAla into a peptide sequence through a synthetic methodology based on the oxidative amidation of conjugated olefins.[8] Specifically, the reaction involved two peptide segments, one requiring a glycinamide at the C-terminus and the other an acryloyl group at the N-terminus. Although successful, such a strategy suffers from limitations, the most important being that it allows the in situ generation of only a single Δ^ZβAla residue within a peptide sequence. Here, we report a novel and more versatile synthetic approach suitable for the stepwise incorporation of multiple Δ^ZβAla units, even consecutively, in peptides. The processes of *Z*−*E* and *E*−*Z* photoisomerization and the properties of the resulting foldamers are also described.

To achieve multiple insertions of Δ^ZβAla residues into a peptide sequence, a derivative compatible with the multistep chemical strategy involved in the solution protocol for peptide synthesis was needed, owing to the intrinsic instability of the unprotected amine group conjugated to the unsaturated C═C bond that does not tolerate removal of any N-protecting group. Compound **8** [*exo*-3-*tert*-butoxycarbonylamino-7-oxabicyclo-(2.2.1)hept-5-ene-*exo*-2-carboxylic acid] was selected as our Δ^ZβAla precursor (Figure 1a). In this compound, the olefinic C═C bond is masked by the formal cycloaddition of furan to Boc-Δ^ZβAla-OH, therefore allowing removal of the Boc group to produce a stable amino derivative. Following our protocol, the cycloaddition of furan (**1**) to maleic anhydride (**2**) afforded selectively the *syn* (*exo*) cycloadduct (**3**), which was subsequently converted to the racemic form of (*exo*,*exo*) cycloadduct **5a** (R = CH_3) or **5b** (R = CH_2CH_3) after a few synthetic steps, namely, monoesterification (yielding **4a** and **4b**) and acyl azide formation followed by a Curtius rearrangement carried out in the presence of *tert*-butyl alcohol

Received: April 18, 2019

DOI: 10.1021/acs.orglett.9b01360
Org. Lett. XXXX, XXX, XXX−XXX

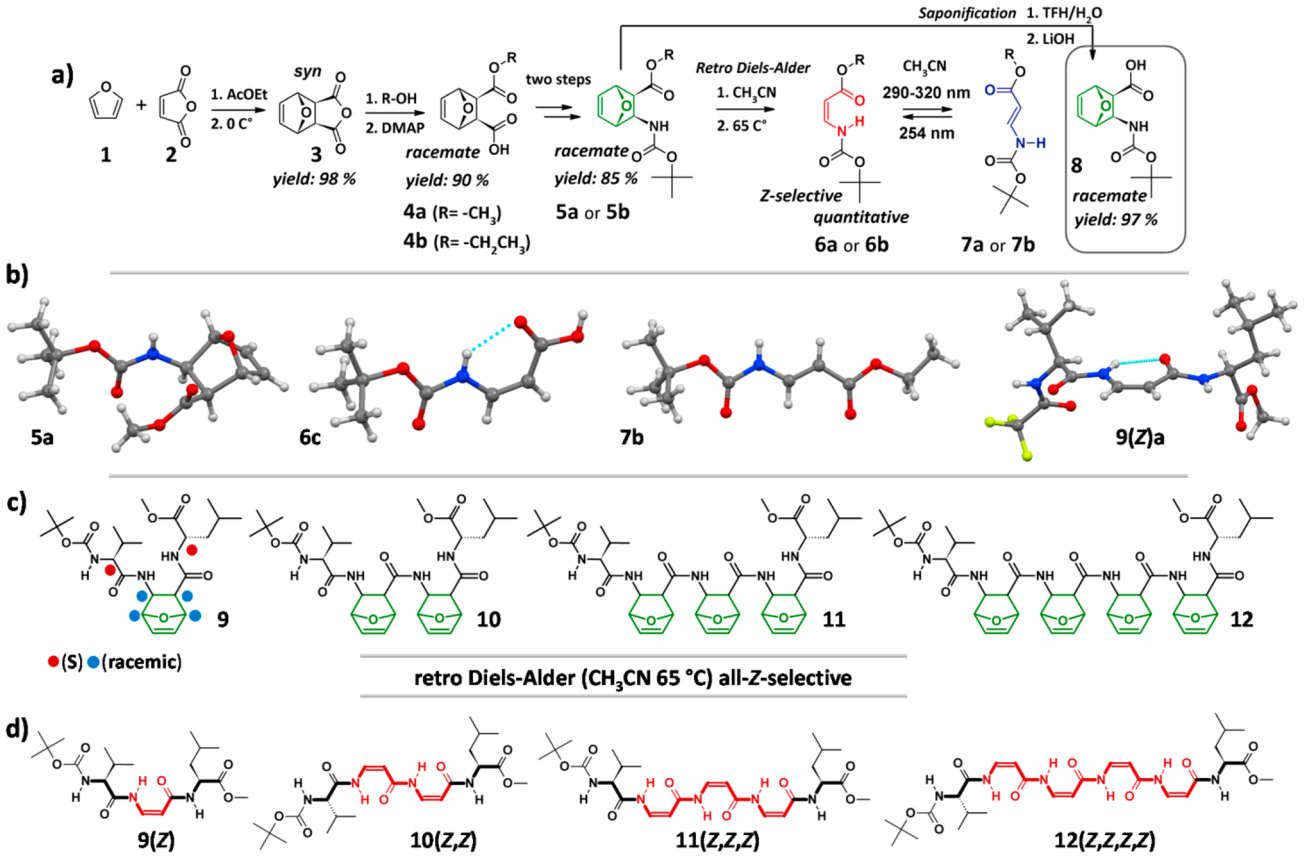

Figure 1. (a) Synthesis of Boc-fm$\Delta^Z\beta$Ala-OH (**8**) and $\Delta^Z\beta$Ala/$\Delta^E\beta$Ala photoconversion. (b) X-ray diffraction structures of **5a**, **6c**, **7b**, and **9**(*Z*)**a**. Intramolecular hydrogen bonds are indicated by dashed lines. (c) Chemical structures of foldamers built by incorporation of consecutively coupled fm$\Delta^Z\beta$Ala residues. (d) Chemical structures of the synthesized foldamers characterized by a row of one to four consecutive $\Delta^Z\beta$Ala residues.

and *p*-toluenesulfonic acid as the catalyst (70% overall yield). By heating **5a** and **5b** in acetonitrile, we obtained Boc-$\Delta^Z\beta$Ala-OR (**6a** and **6b**) quantitatively via the retro-Diels–Alder mechanism. Upon irradiation at 290–320 nm (UV-B), **6a** and **6b** were quantitatively converted to the Boc-$\Delta^E\beta$Ala-OR isomer (**7a** and **7b**).

The back-conversion was achieved in 75% yield by irradiation at 254 nm. Finally, precursor **8** (Boc-fm$\Delta^Z\beta$Ala-OH, where fm stands for furan masking of the olefinic double bond) was obtained after saponification of **5a** and **5b**. The stereochemical output of this series of reactions (see the Supporting Information for NMR spectra) was verified by single-crystal X-ray diffraction analysis of compounds **5a**, **6c**, and **7b**. Analysis of **5a** (Figure 1b) unambiguously confirms the *syn,syn* (*exo,exo*)-type structure of the resulting racemic cycloadduct.[9] The structure of Boc-$\Delta^Z\beta$Ala-OH (**6c**, obtained after saponification of **6a** and **6b**) shows the occurrence of an intramolecular N–H···O=C H-bond that closes a six-atom pseudocycle (C_6 structure) (Figure 1b), made possible by the almost exact (within 1.0°) *trans*, *cis*, and *trans* arrangement of the ϕ, θ, and ψ backbone torsion angles (rotations about the N–C^β, C^β=C^α, and C^α–C bonds, respectively) of $\Delta^Z\beta$Ala. Finally, in **7b** the molecule is perfectly flat in that all non-H atoms, except two methyl carbons of the Boc group, lay on the same plane (Figure 1b) and the value of all backbone torsion angles is 180°. The results described above prompted us to plan the synthesis of foldamers in which $\Delta^Z\beta$Ala would be combined with α-amino acid residues characterized by a good propensity to adopt the β-sheet conformation, namely, Val and Leu. Accordingly, starting from H-Leu-OMe, through a series of conventional peptide couplings (each involving either **8** or a Boc-protected α-amino acid) and Boc deprotection steps, a set of oligomers containing up to four consecutively coupled fm$\Delta^Z\beta$Ala residues were prepared. Because **8** was used in its racemic form while all α-amino acids were of the *S* configuration, each foldamer was obtained as a mixture of diastereomers [compounds **9**–**12** (Figure 1c)]. However, upon thermal treatment of these mixtures to induce retro-Diels–Alders reaction (which proceeded with quantitative *Z* stereoselectivity and yield), restoration of the $\Delta^Z\beta$Ala C=C double bond removed the chiral heterogeneity. The synthesized peptide foldamers comprised a set of compounds of the general sequence Boc-Val-$(\Delta^Z\beta\text{Ala})_n$-Leu-OMe [$n$ = 1, **9**(Z,Z); n = 2, **10**(Z,Z); n = 3, **11**(Z,Z,Z); n = 4, **12**(Z,Z,Z,Z)] characterized by a row of one to four consecutive $\Delta^Z\beta$Ala residues flanked by one α-amino acid at each end (Figure 1d). An analogue of **9**(*Z*) in which Boc protection is replaced by a trifluoroacetyl group was also synthesized, and its structure determined by X-ray diffraction [Figure 1b, structure **9**(*Z*)**a**]. The conformation of the central $\Delta^Z\beta$Ala residue closely matches that reported above for the Boc-protected derivative **6a**, giving rise to an intraresidue N–H···O=C H-bond (C_6 structure) internal to the tripeptide backbone. However, the N–H groups of Val(1) and Leu(3) are oriented nearly perpendicular to each other, and the same holds true for the corresponding carbonyl groups. Such a disposition of the potential intermolecular H-bonding donors and acceptors, combined with the inaccessibility of the N–H and C=O

DOI: 10.1021/acs.orglett.9b01360
Org. Lett. XXXX, XXX, XXX–XXX

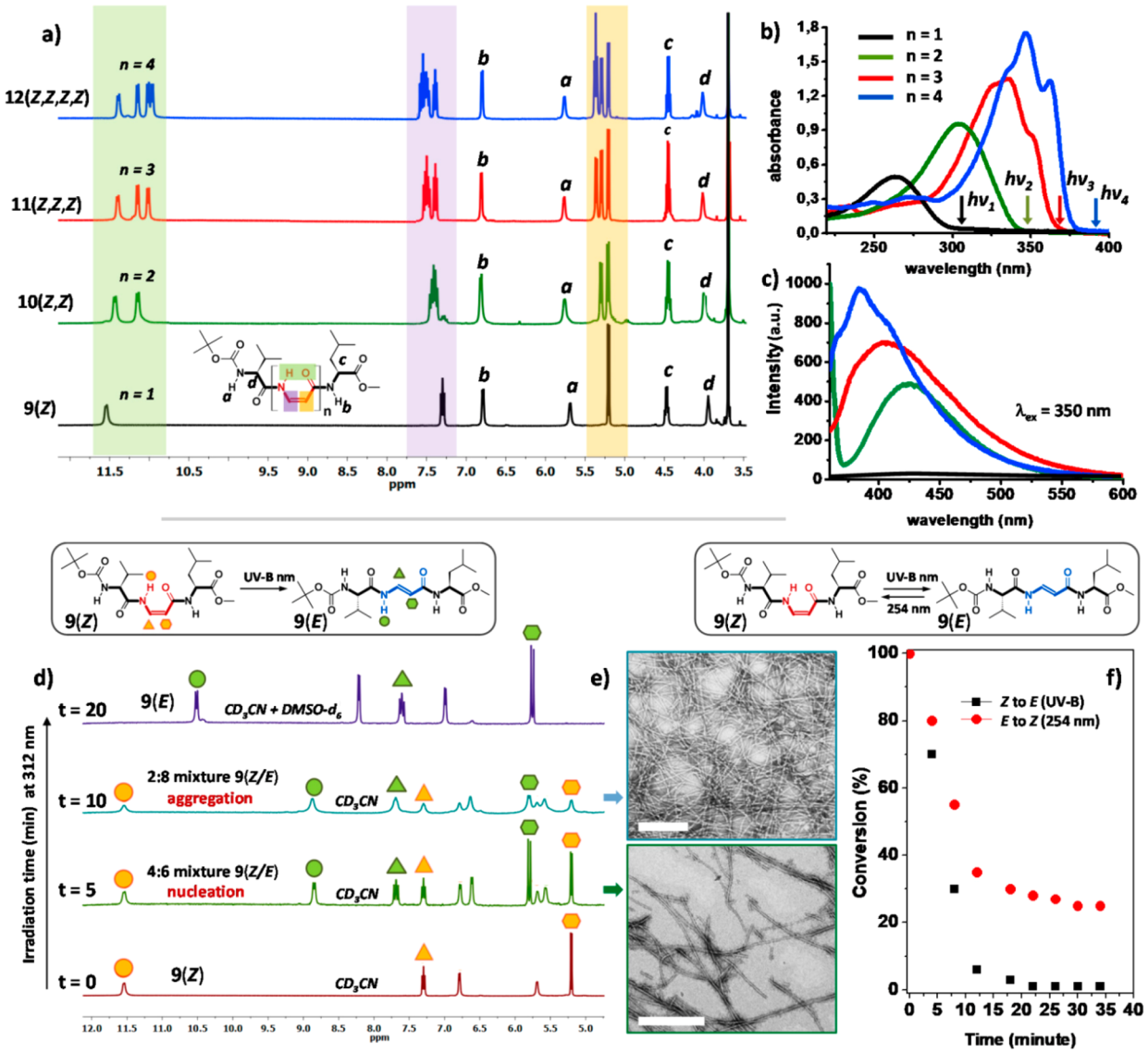

Figure 2. (a) ^{1}H NMR spectra of Boc-Val-($\Delta^Z\beta$Ala)$_n$-Leu-OMe [n = 1−4; **9**(**Z**), **10**(**Z,Z**), **11**(**Z,Z,Z**), and **12**(**Z,Z,Z,Z**), respectively] (peptide concentration of 3 mM in CD_3CN). NH protons involved in an intraresidue H-bond are highlighted in green, while α- and β-olefinic protons are highlighted in orange and purple, respectively. (b and c) UV−vis absorption spectra and fluorescence emission (λ_{ex} at 350 nm), respectively, of Boc-Val-($\Delta^Z\beta$Ala)$_n$-Leu-OMe (n = 1−4). (d) ^{1}H NMR spectra of **9**(**Z**)−**9**(**E**) isomerization recorded under different periods of exposition during UV-B illumination. Proton signals belonging to $\Delta^Z\beta$Ala and $\Delta^E\beta$Ala units are highlighted. (e) TEM images recorded for 4:6 (bottom) and 2:8 (top) **9**(**Z**)/**9**(**E**) isomeric mixtures (scale bar of 100 nm, stained samples). (f) Kinetics of **9**(**Z**)−**9**(**E**) (UV-B, black squares) and **9**(**E**)−**9**(**Z**) (254 nm, red circles) photoconversions (data from HPLC).

groups of $\Delta^Z\beta$Ala (already intramolecularly engaged), hampers the possibility that intermolecular H-bonding may give rise to a sheetlike arrangement in the crystal packing.

The ^{1}H NMR spectra of the foldamers belonging to the Boc-Val-($\Delta^Z\beta$Ala)$_n$-Leu-OMe series (n = 1−4; 2 mM in CH_3CN) are reported in Figure 2a. The NH proton of each $\Delta^Z\beta$Ala residue is found in the low-field spectral region, indicative of its involvement in an intraresidue (C_6) H-bond. As a function of foldamer elongation in the Boc-Val-($\Delta^Z\beta$Ala)$_n$-Leu-OMe series, a remarkable red-shift of the maximum is observed in the corresponding UV−vis absorption spectra (Figure 2b), from 260 nm (n = 1) to 310 nm (n = 2), 337 nm (with a shoulder at 362 nm) (n = 3), and 350 nm (with a shoulder at 370 nm) (n = 4). The increasing number of consecutive $\Delta^Z\beta$Ala residues in the foldamer backbone seems to give rise to a progressively expanded, conjugated π-system involving both olefin and amide groups. Such a conjugation is expected to be maximized if all $\Delta^Z\beta$Ala residues adopt a conformation similar to that found for **6a** and **9**(**Z**)**a** (see above), i.e., a fully planar system. The UV−vis absorption profiles of the **9**(**Z,Z**)−**12**(**Z,Z,Z,Z**) series suggested that we explore a set of different wavelengths ($h\nu$ as reported in Figure 2b) to induce the photoisomerization of these foldamers to their corresponding E isomers and for the reverse process, as well. Clearly, on the way from the all-Z to all-E isomeric states of the -($\Delta\beta$Ala)$_n$- oligomers, when n > 1 additional combinations of isomeric forms are also implicated, for a total of 2^n isomers. The **9**(**Z**) → **9**(**E**) isomerization was monitored by NMR spectroscopy (Figure 2d, red trace). Experimental condition: 3 mM **9**(**Z**) in CD_3CN, quartz NMR tube.

After irradiation under UV-B light for 5 min, the new isomer **9**(**E**) started to form, yielding a **9**(**Z**)/**9**(**E**) mixture in 4:6

DOI: 10.1021/acs.orglett.9b01360
Org. Lett. XXXX, XXX, XXX−XXX

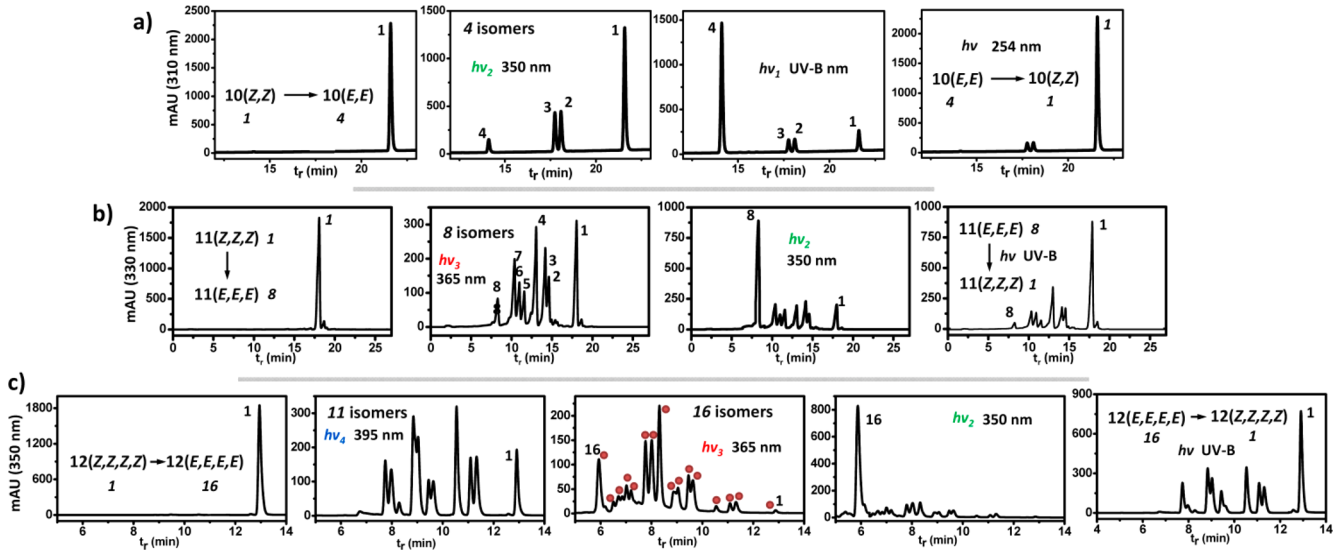

Figure 3. (a–c) HPLC profiles of the photoconversion process from the all-*Z* isomer to mainly the all-*E* isomer starting from **10**(*Z*,*Z*), **11**(*Z*,*Z*,*Z*), and **12**(*Z*,*Z*,*Z*,*Z*), respectively. Solvent MeOH, concentrations of 5 μM for all samples. The HPLC profiles reported at the right of each row show the corresponding all-*E*–all-*Z* back-isomerization process.

molar ratio (determined by HPLC), which gave rise to a weak organogel state (Figure 2d, green trace, and corresponding TEM image). Irradiation for an additional 5 min generated a **9**(*Z*)/**9**(*E*) mixture in a 2:8 molar ratio (by HPLC), which turned the NMR trace in a set of broad NMR proton signals and in a robust organogel state (Figure 2d, blue trace, and corresponding TEM image). After addition of DMSO-d_6 to the CD_3CN solution, the organogel collapsed to a liquid state, and upon irradiation for an additional 10 min, the isomerization process produced **9**(*E*) in quantitative yield (Figure 2d, violet trace). TEM analyses clearly show how the progressive formation of ordered supramolecular fibers is related to the incremental conversion of **9**(*Z*) to **9**(*E*) (Figure 2e). The latter compound at the critical concentration of 2.4 mM (referenced to its own concentration in the mixture) was the origin of a dense fiber network that could entrap the solvent (acetonitrile). The reversible **9**(*E*) → **9**(*Z*) conversion was achieved by irradiation at 254 nm (Figure 2e, experiments run in MeOH to avoid aggregation). While the **9**(*Z*) → **9**(*E*) transformation occurred quantitatively, the back process **9**(*E*) → **9**(*Z*) reached a photostationary equilibrium at 77% conversion. In our view, the strong tendency of **9**(*E*) to self-associate into fibers, at variance with its **9**(*Z*) counterpart, might arise from an extended conformation adopted by $\Delta^E\beta$Ala (similar to that described above for **7** in the crystal state), combined with the availability for intermolecular H-bonding of an additional NH group free from intramolecular interactions.

As for the higher oligomers, we found that photoconversions from the all-*Z* isomer to a mixture in which the all-*E* isomer was by far the most abundant component required successive irradiation steps at different wavelengths. On the basis of the UV–vis absorption profiles of Boc-Val-$(\Delta^Z\beta\text{Ala})_n$-Leu-OMe ($n$ = 1–4) reported in Figure 2b, we selected four wavelengths (indicated by arrows in Figure 2b) that fall each in the red tail of the absorption profile of one of the compounds: irradiation at 350 nm, followed by UV-B, for **10**(*Z*,*Z*); 365 nm, followed by 350 nm, for **11**(*Z*,*Z*,*Z*); and 395 nm, followed by 365 nm and successively by 350 nm, for **12**(*Z*,*Z*,*Z*,*Z*) (Figure 3a–c, respectively). Indeed, on the way from the all-*Z* to the all-*E* isomers, a mixture of isomers in which *Z* and *E* units are variously combined is likely to be formed, somehow resembling the conjugation state of some of the lower all-*Z* homologues. These latter require progressively higher irradiation energies for their *Z*–*E* conversion as the number of consecutive *Z* units decreases. It is noteworthy that these processes can be achieved in high conversion yields (as shown in the reported HPLC profiles) when concentrations are <5 μM. These conditions are required because of the strong aggregation tendency of **10**(*E*,*E*)–**12**(*E*,*E*,*E*,*E*) and their mixed intermediate species. All HPLC peaks were found to be *iso* mass with the corresponding precursors. Interestingly, if compared to their all-*Z* counterparts, foldamers **10**(*E*,*E*), **11**(*E*,*E*,*E*), and **12**(*E*,*E*,*E*,*E*) are characterized by blue-shifted UV–vis absorption profiles (see the Supporting Information), accompanied by a loss of fluorescence. The back-isomerization process was also investigated [from all-*E* to all-*Z* isomers (Figure 3a–c, right HPLC profiles)]. High levels of conversion were found in the case of **10**(*Z*,*Z*) (at 254 nm) and **11**(*Z*,*Z*,*Z*) (at UV-B), while moderate conversion was achieved in the case of **12**(*Z*,*Z*,*Z*,*Z*). All compounds after reconversion to their corresponding all-*Z* isomers restored the native fluorescence.

To summarize, foldamers featuring consecutive $\Delta^Z\beta$Ala/$\Delta^E\beta$Ala units are endowed with interesting conformational, electronic, and supramolecular aggregation properties that can be modulated by selective *E*–*Z* photoisomerization. The synthetic route developed in this work offers possibilities for the exploitation of the $\Delta^Z\beta$Ala/$\Delta^E\beta$Ala dyad in photoresponsive systems.

■ ASSOCIATED CONTENT

Supporting Information

The Supporting Information is available free of charge on the ACS Publications website at DOI: 10.1021/acs.orglett.9b01360.

Experimental details, X-ray crystallographic data, spectroscopic data for new compounds, and additional figures (PDF)

DOI: 10.1021/acs.orglett.9b01360
Org. Lett. XXXX, XXX, XXX–XXX

Accession Codes

CCDC 1901757−1901760 contain the supplementary crystallographic data for this paper. These data can be obtained free of charge via www.ccdc.cam.ac.uk/data_request/cif, or by emailing data_request@ccdc.cam.ac.uk, or by contacting The Cambridge Crystallographic Data Centre, 12 Union Road, Cambridge CB2 1EZ, UK; fax: +44 1223 336033.

AUTHOR INFORMATION

Corresponding Author

*E-mail: alessandro.moretto.1@unipd.it.

ORCID

Marco Crisma: 0000-0003-3552-4106
Alessandro Moretto: 0000-0003-1563-9053

Notes

The authors declare no competing financial interest.

ACKNOWLEDGMENTS

The work was funded by the CARIPARO Foundation (Ph.D. program, Padova, Italy), the Italian Ministero dell'Istruzione, dell'Università e della Ricerca (MIUR) (Grant PRIN 20157WW5EH), and the University of Padova (Grant P-DiSC 06BIRD2018-UNIPD).

REFERENCES

(1) Gellman, S. H. *Acc. Chem. Res.* **1998**, *31*, 173−180.

(2) (a) Toniolo, C.; Crisma, M.; Formaggio, F.; Peggion, C. *Biopolymers* **2001**, *60*, 396−419. (b) Hecht, S.; Huc, I. *Foldamers: Structure, Properties and Applications*; Wiley-VCH: Weinheim, Germany, 2007. (c) Goodman, C. M.; Choi, S.; Shandler, S.; DeGrado, W. F. *Nat. Chem. Biol.* **2007**, *3*, 252−262. (d) Seebach, D.; Gardiner, J. *Acc. Chem. Res.* **2008**, *41*, 1366−1375. (e) Horne, W. S.; Gellman, S. H. *Acc. Chem. Res.* **2008**, *41*, 1399−1408. (f) Saraogi, I.; Hamilton, A. D. *Chem. Soc. Rev.* **2009**, *38*, 1726−1743. (g) Li, Z. T.; Hou, J. L.; Li, C. *Acc. Chem. Res.* **2008**, *41*, 1343−1353. (h) Martinek, T. A.; Fülöp, F. *Chem. Soc. Rev.* **2012**, *41*, 687−702.

(3) Le Bailly, B. A. F.; Clayden, J. *Chem. Commun.* **2016**, *52*, 4852−4863.

(4) (a) Peggion, C.; Crisma, M.; Toniolo, C.; Formaggio, F. *Tetrahedron* **2012**, *68*, 4429−4433. (b) Crisma, M.; Saviano, M.; Moretto, A.; Broxterman, Q. B.; Kaptein, B.; Toniolo, C. *J. Am. Chem. Soc.* **2007**, *129*, 15471−15473.

(5) (a) De Poli, M.; Zawodny, W.; Quinonero, O.; Lorch, M.; Webb, S. J.; Clayden, J. *Science* **2016**, *352*, 575−580. (b) Le Bailly, B. A. F.; Byrne, L.; Clayden, J. *Angew. Chem., Int. Ed.* **2016**, *55*, 2132−2136. Lister, F. G. A.; Le Bailly, B. A. F.; Webb, S. J.; Clayden, J. *Nat. Chem.* **2017**, *9*, 420−425.

(6) Mazzier, D.; Crisma, M.; De Poli, M.; Marafon, G.; Peggion, C.; Clayden, J.; Moretto, A. *J. Am. Chem. Soc.* **2016**, *138*, 8007−8018.

(7) For examples of photoisomerizable systems, see: (a) Wang, L.; Li, Q. *Chem. Soc. Rev.* **2018**, *47*, 1044−1097. (b) Feringa, B. L. *Angew. Chem., Int. Ed.* **2017**, *56*, 11059−11078. (c) Bandara, H. M. D.; Burdette, S. C. *Chem. Soc. Rev.* **2012**, *41*, 1809−1825. (d) Yu, Z.; Hecht, S. *Angew. Chem., Int. Ed.* **2011**, *50*, 1640−1643. (e) Amirjalayer, S.; Martinez-Cuezva, A.; Berna, J.; Woutersen, S.; Buma, W. J. *Angew. Chem., Int. Ed.* **2018**, *57*, 1792−1796. (f) Wang, H.; Bisoyi, H. K.; Wang, L.; Urbas, A. M.; Bunning, T. J.; Li, Q. *Angew. Chem., Int. Ed.* **2018**, *57*, 1627−1631. (g) Irie, M. *Chem. Rev.* **2000**, *100*, 1685−1716. (h) Han, D.; Jiang, B. L.; Feng, J.; Yin, Y. D.; Wang, W. S. *Angew. Chem., Int. Ed.* **2017**, *56*, 7792−7796. (i) Yoon, J.; de Silva, A. P. *Angew. Chem., Int. Ed.* **2015**, *54*, 9754−9756.

(8) Marafon, G.; Crisma, M.; Moretto, A. *Angew. Chem., Int. Ed.* **2018**, *57*, 10217−10220.

(9) The X-ray diffraction structure of the *endo,exo* diastereomer of **5b** was previously reported. See: Masesane, I. B.; Batsanov, A. S.; Howard, J. A. K.; Mondal, R.; Steel, P. G. *Beilstein J. Org. Chem.* **2006**, *2*, 9.

DOI: 10.1021/acs.orglett.9b01360
Org. Lett. XXXX, XXX, XXX−XXX